

Metal-Enhanced Fluoroimmunoassay on a Silver Film by Vapor Deposition

Jian Zhang, Evgenia Matveeva, Ignacy Gryczynski, Zoya Leonenko, and Joseph R. Lakowicz*

Center for Fluorescence Spectroscopy, Department of Biochemistry and Molecular Biology, University of Maryland School of Medicine, 725 West Lombard Street, Baltimore, Maryland 21201

Received: September 22, 2004; In Final Form: December 2, 2004

We studied a fluoroimmunoassay using metal-enhanced fluorescence (MEF) detection on silver film generated by vapor deposition method. The morphology of the silver film was controlled through the thickness of the film. A silica layer was coated on the silver film to protect the film and separate the fluorophore from the metal surface. Rabbit immunoglobulin G (IgG) was adsorbed on the silica by physisorption and then dye-labeled anti-rabbit IgG was bound to the immobilized rabbit IgG. It was observed that the fluorophore was quenched on a thin silver film (2 nm), enhanced on a thick film (>5 nm), and reached saturation (ca. 10 times enhancement) at 20 nm. The MEF was also dependent on the thickness of the silica with a maximum at 10 nm. The lowest lifetime was observed on the 20 nm silver film, which was consistent with the saturation of MEF. These results showed the properties of a silver film needed for a maximum increase of fluorescence intensity in a fluoroimmunoassay. Dependence of the MEF on the emission wavelength was also studied using different dye-labeled anti-rabbit IgGs.

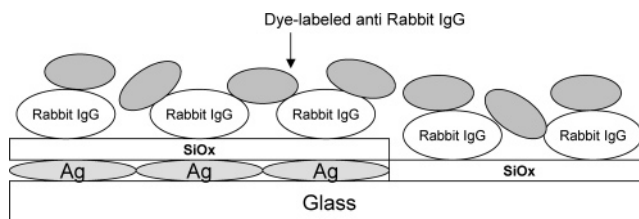
Introduction

Fluorescence is an important tool for biological analysis.^{1–3} Fluorescence intensity can be enhanced by an order of magnitude or more when a fluorophore is nearby a surface of silver nanostructure.^{4,5} This effect is known as metal-enhanced fluorescence (MEF).^{6–9} The MEF is principally attributed to the local electromagnetic field, which interacts with incident light and the excited fluorophore. There are absorbing and scattering components in these interactions.^{6,10,11} According to our recently proposed radiating plasmon (RP) model,¹² the emission or quenching for the fluorophore near the surface of the metal nanoparticle can be predicted from its optical properties, which in turn depend on the size and shape of particle.^{12–15}

The MEF technique can be utilized to develop a sensitive immunoassay. In this study, rabbit immunoglobulin G (IgG) was adsorbed on the silver nanostructure by physisorption,^{16–18} and dye-labeled anti-rabbit IgG was bound to the immobilized IgG (Scheme 1).¹⁹ This model fluoroimmunoassay was set to study the dependence of fluorescence enhancement on the morphology of the silver structure. The silver film was coated by varying thicknesses of silica to study the dependence of MEF on the distance between the fluorophore and silver surface as well as to protect the silver film. The enhancement mechanism was discussed on the basis of the lifetime measurement. Different dye-labeled anti-rabbit IgGs were also employed to study the dependence of MEF on the emission wavelength in a range of 550–750 nm. Finally, we wished to find the optimal conditions for the maximum MEF on the fluoroimmunoassay detection.

Silver nanostructure can be generated by versatile methods. Vacuum evaporation was adopted in this study because of its simple operation and good stability in generating a silver film

SCHEME 1: Model Fluoroimmunoassay on a Silver Film



on a solid substrate.^{20–26} The morphology of the silver film, which was important for its optical properties, could be controlled by the thickness of the metal film and the deposition rate.²⁰ The silver film was deposited at a slow rate in this study to result in a rough surface, which was expected to have a good MEF behavior. A silica layer was covered on the silver film in the same chamber.

Experimental Section

Materials. Silicon monoxide and silver wire (99.999%) were purchased from Aldrich. Alexa Fluor-555, Rhodamine 6G, Alexa Fluor-647, Alexa Fluor-680, and Alexa Fluor-750 anti-rabbit IgGs (2 mg/mL) were purchased from Molecular Probes. Rabbit IgG (5 mg/mL), buffer components, and salts (such as bovin serum albumin, glucose, and sucrose) were from Sigma-Aldrich. Nanopure water (> 18.0 M Ω) purified using a Millipore Milli-Q gradient system was used in experiments.

Silver Film by Vacuum Vapor Deposition. Silver films were deposited in a consolidated vacuum vapor deposition system (model 306, Edward).²⁷ Glass slides were pretreated by air plasma under 1×10^{-4} mbar for 3 min before depositing the metal film to increase the stickiness of metal. The silver wire was melted on the filament, evaporated under a pressure of $< 1 \times 10^{-7}$ mbar, and deposited on the glass slide. The deposition rate was adjusted by the filament current, and the thickness of film was measured with a quartz crystal microbalance. Silica

* Author to whom correspondence should be addressed. Phone: (410) 706-8409. Fax: (410) 706-8408. E-mail: lakowicz@cfs.umbi.umd.edu.

layer (SiO_x) was grown on the silver film using silicon monoxide in the same vacuum chamber.

Immunoassay Procedures. The slide was covered with a water-prevented tape with wells of diameter 5 mm. The IgG solution was diluted with sodium phosphate buffer (50 mM, pH = 7.4) to 17 $\mu\text{g}/\text{mL}$. A 25 μL aliquot of diluted IgG solution was added to each well. The slide was incubated for 4 h at room temperature in a humid chamber, then rinsed with water and washing solution (0.05% Tween-20 in water). Blocking was performed by adding 25 μL of blocking buffer (1% bovine serum albumin, 1% sucrose, 0.05% NaN_3 , 0.05% Tween 20 in 50 mM Tris-HCl buffer, pH = 7.4) overnight at 4 °C in a humid chamber. After the slide was washed with water and washing solution, a diluted dye-labeled conjugate solution (10 mg/mL in blocking solution) was added to the well on the slide and incubated in a humid chamber at room temperature for 2 h. After incubation, the residual supernatant solution was collected to detect the fluorophore intensity change before and after the binding. The slide was then rinsed with water, washing solution, and water. After being covered with blocking buffer, the slide was stored at 4 °C before the measurement.

Spectral Measurements. Absorption spectra were monitored with a Hewlett-Packard 8453 spectrophotometer. Fluorescence spectra were recorded with a Cary Eclipse fluorescence spectrophotometer. Surface fluorescence spectra were recorded with an excitation angle of 90° and monitoring angle of 45°. A combination of a fluoroimmunoassay-coated glass slide and a corresponding silver film-coated slide worked as a control to eliminate the reflection effect from the excitation and emission by the silver film. Lifetimes were recorded with a 10 GHz frequency-domain fluorometer^{9a} using a mode-locked argon ion laser at 514 nm, 76 MHz repetition rate, and 120 ps pulse width. Excitation and emission polarizers were in the magic angle orientation. Emission was selected with a combination of a 520 nm long-pass liquid chromate filter ($\text{CrO}_4^{2-}/\text{Cr}_2\text{O}_7^{2-}$, 0.3 M, pH 8) placed in a 2 mm, 1 in. \times 1 in., quartz cuvette and an interference filter at 540 ± 10 nm. Such a combination of filters rejects efficiently scattered light and has minimal internal luminescence.

Atomic Force Microscopy (AFM). AFM images were collected with an atomic force microscope (TMX 2100 Explorer SPM, Veeco), equipped with an AFM dry scanner.^{28,29} Surfaces were imaged in air, in tapping mode of operation, using AFM noncontact-mode cantilevers (Veeco). Samples were freshly prepared prior to imaging. The AFM scanner was calibrated using a standard calibration grid as well as gold nanoparticles 100 nm in diameter from Ted Pella. Images were analyzed using SPMLab software. Statistical height analysis was performed using at least 100 measurements. All statistics were performed in the 95% confidence interval.

Results and Discussion

Surface morphology of the silver film was dependent on its thickness and deposition rate in the preparation.²⁰ A slow deposition rate was expected to result in a rough surface, which led to a stronger metal-enhanced fluorescence (MEF). Therefore, all silver films were deposited at a slow rate of 0.1 nm/10 s in this study. The thicknesses of these silver films, which were monitored by a crystal microbalance, were in a range of 2–120 nm. When the silver films were 2–10 nm thick, they displayed plasmon absorbances at 490–650 nm, indicating that the films were composed of nanoscale particles. The plasmon wavelength was red-shifted with increasing the thickness of the silver film, corresponding to the size increase of particles in the film. The

silver film could not be characterized accurately by the absorbance spectrum when the thickness was above 10 nm.

The surface morphology was detected by the atomic force microscope (AFM). The AFM images showed that a thin silver film (thickness = 10 nm) was composed of compactly packed individual particles (Figure 1a). The three-dimensional (3D) image showed that the height of an adhered particle was 14 nm, close to the *average* thickness of silver film. The particle size was found to increase with the thickness of silver film from 2 to 20 nm, which was consistent with the results obtained from the absorbance spectra. The surface became continuous and rough when the silver film was thicker than 20 nm (Figure 1b, thickness = 50 nm), and its 3D image showed a close thickness measured by the microbalance.

We studied the dependence of MEF on the thickness of the silver film. To avoid a strong quenching of the fluorophore due to the close proximity of fluorophore to the metal surface as well as to protect the silver film, a 5 nm silica layer (written as SiO_x because of its mixed composition of SiO_2 and SiO) was coated on the silver film by the vapor deposition in the same chamber. Rabbit IgG was adsorbed by physisorption on the silica,¹⁹ which could be verified by the AFM image. A glass substrate was expected to display an analogous feature to the silica and was used to immobilize the IgG. Some spots were observed on the smooth glass surface, and the heights of these spots were 5–10 nm (Figure 1c). The IgG molecule was described as a cylinder shape with a 4 nm diameter and a 10 nm height, consistent with the shape of these spots, so the spots were attributed to the immobilized IgG molecules. Alexa Fluor-555 anti-rabbit IgG were bound to the immobilized IgG on the solid substrate. The bound Alexa Fluor-555 anti-rabbit IgG could be verified by the surface luminescence upon excitation at 514 nm. The concentration of bound fluorophore could be estimated quantitatively through the luminescence difference in the buffer solution before and after binding. Because there were an *average* of 4.5 fluorophores on one antibody molecule, the antibody coverage on the silica was estimated to be ca. 1×10^{-12} mol/ cm^2 . It was known that one IgG molecule could bind 1–2 antibody molecules, so the coverage of IgG molecules was inferred to be less than 2×10^{-12} mol/ cm^2 . This coverage was found to be almost independent of the thickness of the silver film or silica layer.

The wells on the slides were immersed with buffer solution, and the bound fluorophore displayed an emission wavelength at 568 nm upon excitation at 514 nm, close to that of the free fluorophore in buffer solution (563 nm). Relative to the intensity on the glass substrate, the fluorescence brightness from the labeled antibody on the silver film became darker when the thickness was 2 nm, then increased to be close to that on the glass substrate when the thickness increased to 5 nm (Figure 2). Fluorescence on the 10 nm silver film was enhanced about 2 times. The enhancement factor, which was defined as the ratio of intensity on the metal film over that on the glass substrate, was plotted against the thickness of silver film, showing that the enhancement factor was lower than one at 2 nm thickness, increased with the thickness, and then reached saturation at 20 nm thickness (Figure 3). It was hence concluded that the MEF displayed a quenching on a thin silver film and enhancement on a thick silver film.

According to our recently proposed radiating plasmon (RP) model,¹⁴ the emission or quenching of a fluorophore near the surface of metal nanoparticles can be predicted from their optical properties. The extinction properties of metal particles can be expressed by a combination of both absorption (C_A) and

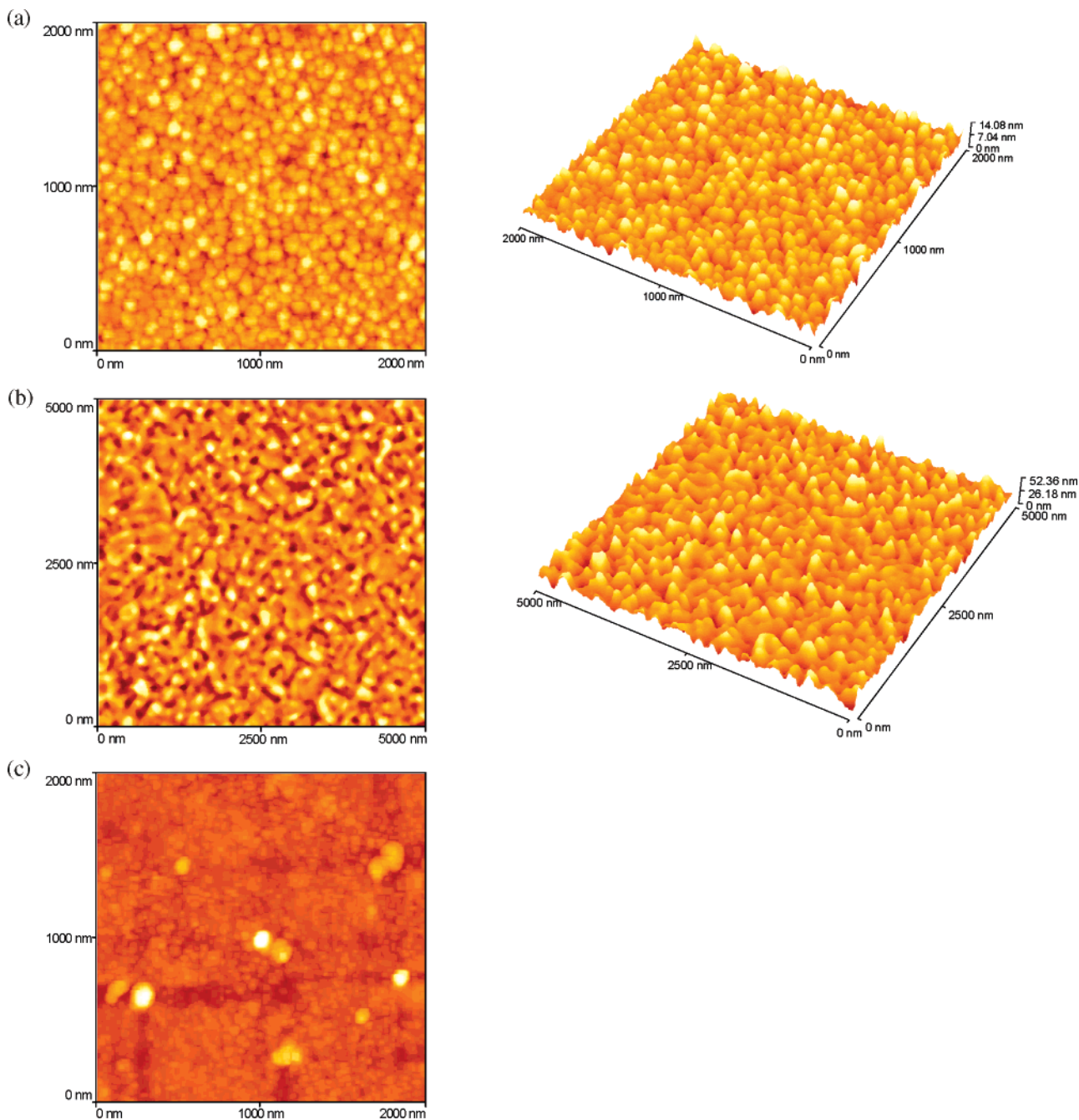


Figure 1. AFM images. (a) A 10 nm thickness of silver film and its 3D image. (b) A 50 nm thickness of silver film and its 3D image, and (c) IgG on the glass substrate.

scattering (C_S) factors when the particles are spherical and have a comparable size to the incident wavelength¹²

$$C_E = C_A + C_S = k_1 \text{Im}(\alpha) + \frac{k_1^4}{6\pi} \quad (1)$$

where $k_1 = 2\pi n_1/\lambda_0$ is the wave vector of the incident light in medium 1 and α is the polarizability of the sphere of radius r

$$\alpha = 4\pi r^3(\epsilon_m - \epsilon_1)(\epsilon_m + 2\epsilon_1) \quad (2)$$

and ϵ_m is the complex dielectric constant of metal. The first term represents the cross section due to absorption, and the second term represents the cross section due to scattering. We expected C_A to cause quenching and C_S to cause enhancement.¹² The quenching term increases as a r^3 factor, and the enhance-

ment term increases as a r^6 factor. Examinations of C_A and C_S calculated from Mie theory show that the small metal particles are expected to quench fluorescence because the absorption dominates over the scattering, while the larger size nanostructures are expected to enhance fluorescence because the scattering component is dominant over the absorption.^{7,13} In this study, the thin film was composed of small particles, while the particle size became large with increasing the thickness. Therefore, it was plausible that the thin silver film displayed only a quenching and a thick silver film displayed an enhancement. The MEF also became stronger with increasing the thickness of silver film.

The distance from fluorophore to the surface of the silver film is also an important factor relevant to the MEF.⁵ In this study, the 10 nm thick silver film was coated with a varying thickness of silica in a range of 0–50 nm. The enhancement factor was observed to increase with the thickness and reach

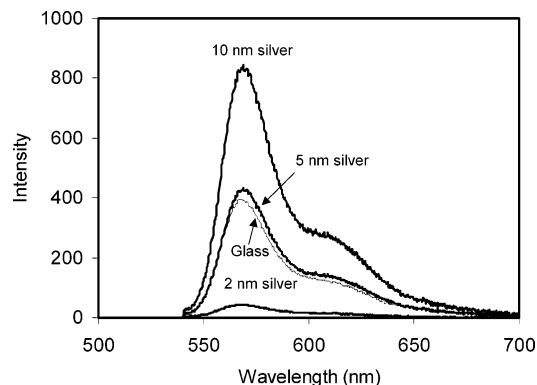


Figure 2. Surface emission spectra of bound Alexa Fluor-555 labeled antibody on varying thicknesses of silver films including 2, 5, and 10 nm as well as on the glass substrate.

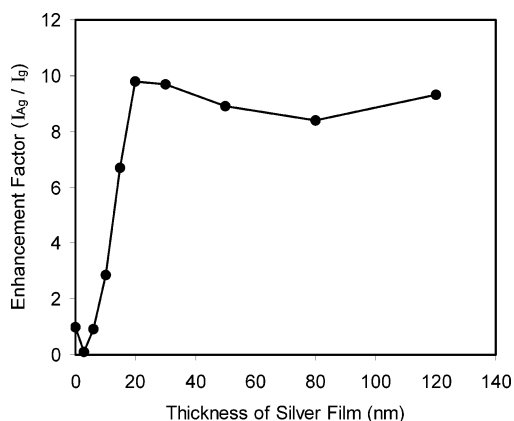


Figure 3. Dependence of the enhancement factor on the thickness of silver film coated by a 5 nm thickness of silica upon excitation at 514 nm.

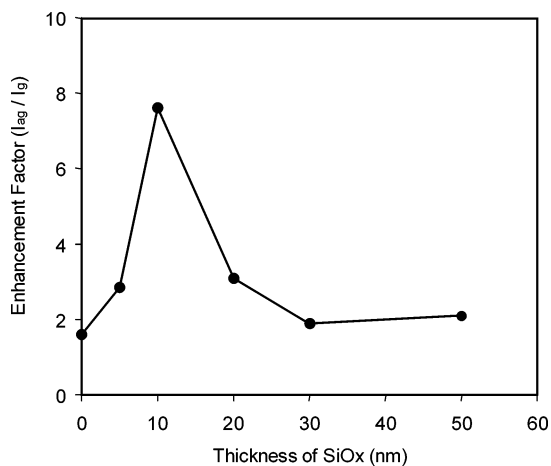


Figure 4. Dependence of the enhancement factor on the thickness of silica coated on a 10 nm thickness of silver film.

the maximum at 10 nm (Figure 4). The IgG molecule was described as a cylinder shape with a 4 nm diameter and a 10 nm height, so the thickness of the immunoassay was regarded to be ca. 4–10 nm. With a combination of the thickness of silica and the immunoassay, the distance of the maximum MEF was ca. 14–20 nm, close to that obtained experimentally on the silver islands made by a chemical reaction^{5a} or from the local electromagnetic field on silver particle.¹⁰ The enhancement factor decreased with the thickness of the silica when it was more than 10 nm and was only about 2 at 50 nm, implying that

TABLE 1: Lifetime Data Obtained Using the Multiexponential Model for the Fluorophore Coated on the Glass Substrate or Silver Surface

Ag/silica (nm)	τ_i (ns)	f_i	α_i	$\bar{\tau}$ (ns)	$\langle \tau \rangle$ (ns)	χ^2
glass substrate	0.061	0.022	0.175	0.661	0.487	1.10
	0.291	0.203	0.339			
	0.776	0.775	0.486			
5/5	0.028	0.241	0.797	0.327	0.390	2.11
	0.243	0.429	0.166			
	0.845	0.330	0.037			
20/5	0.038	0.447	0.837	0.205	0.071	0.94
	0.198	0.414	0.149			
	0.756	0.140	0.013			
50/5	0.060	0.063	0.311	0.459	0.280	1.53
	0.242	0.319	0.390			
	0.617	0.618	0.298			
10/0	0.003	0.398	0.975	0.189	0.008	2.21
	0.129	0.392	0.023			
	0.651	0.210	0.002			
10/10	0.018	0.594	0.921	0.154	0.027	1.14
	0.116	0.330	0.078			
	1.38	0.076	0.001			
10/20	0.040	0.125	0.659	0.577	0.213	1.50
	0.320	0.270	0.180			
	0.802	0.606	0.161			
10/50	0.098	0.052	0.243	0.610	0.457	0.57
	0.460	0.581	0.577			
	0.934	0.367	0.180			

this distance was too large for an efficient MEF. Hence, the optimal distance for the maximum MEF was ca. 10 nm in this fluoroimmunoassay model on the silver film by the vapor deposition method.

It is known that the fluorophore near the metal surface is strongly quenched by the metallic surface but enhanced when beyond the quenching region.⁶ This enhancement depends on the increase of the intrinsic decay rate of the fluorophore, which can be described by lifetime. The lifetime hence is an important factor to determine the MEF mechanism. In our experiments, the frequency-domain (FD) intensity decays were analyzed in terms of the multiexponential model⁵

$$I(t) = \sum_i \alpha_i \exp(-t/\tau_i) \quad (3)$$

where α_i are the amplitudes and τ_i are the decay times, $\sum \alpha_i = 1.0$. The fractional contribution of each component to the steady-state intensity is given by

$$f_i = \frac{\alpha_i \tau_i}{\sum_i \alpha_i \tau_i} \quad (4)$$

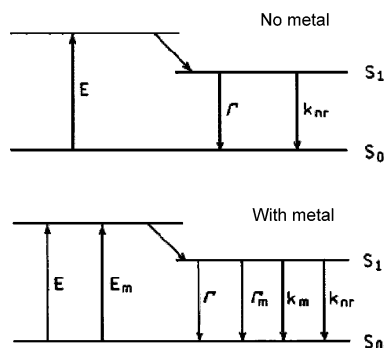
The mean lifetime of the excited state is given by

$$\bar{\tau} = \sum_i f_i \tau_i \quad (5)$$

and the amplitude-weighted lifetime is given by

$$\langle \tau \rangle = \sum_i \alpha_i \tau_i \quad (6)$$

The values of α_i and τ_i were determined by a nonlinear least-squares impulse deconvolution with a goodness-of-fit χ^2_R criterion. After being fit to the multiexponential model, the lifetimes were obtained and listed in Table 1. It was shown that the lifetime of fluorophore on the silver film was shorter than

SCHEME 2: Jablonski Diagram for Free Fluorophores (Top) and on Silver Film (Bottom)


that on the glass substrate because of its higher intrinsic decay rate. The lifetime was dependent on the thickness of silver film, which was consistent with the distance of saturation MEF. Meanwhile, the lifetime was also dependent on the thickness of silica coated on the silver film, and the shortest lifetime was at a 10 nm thickness of silica, exactly corresponding to the maximum MEF. When the silica was 50 nm thick, the lifetime was close to that on the glass substrate, implying that the interaction between the fluorophore and silver film was weak at this distance. This result was also verified by the fluorescence intensity change. For all samples, the shortest lifetime was on a bare silver surface without silica, which was due to the quenching.

This enhancement depends on two major factors, an enhanced local electromagnetic field and an increase of the intrinsic decay rate of the fluorophore.⁶ The first factor provides stronger excitation rates, and the second one changes quantum yield and lifetime. The observed fluorescence enhancement factor (G) hence can be written as the product of two factors, excitation (G_{ex}) and quantum yield (G_{QY})⁶

$$G \approx G_{\text{ex}} G_{\text{QY}} \quad (7)$$

where $G_{\text{QY}} = Q_{\text{m}}/Q_0$ is the increase in quantum yield. The energy diagrams were shown for the fluorophore on the glass or on the silver film (Scheme 2).⁴ On the glass substrate, the quantum yield (Q_0) and lifetime (τ_0) are given by

$$Q_0 = \Gamma/(\Gamma + k_{\text{nr}}) \quad (8)$$

$$\tau_0 = 1/(\Gamma + k_{\text{nr}}) \quad (9)$$

where Γ is a radiative rate and k_{nr} is a nonradiative decay rate. In this experiment, the Q_0 and τ_0 can be regarded as those of the fluorophore on the glass substrate. For the fluorophore on the metal surface, the quantum yield (Q_{m}) and lifetime (τ_{m}) are given by eqs 10 and 11

$$Q_{\text{m}} = \frac{\Gamma + \Gamma_{\text{m}}}{\Gamma + \Gamma_{\text{m}} + k_{\text{nr}} + k_{\text{m}}} = \frac{\Gamma(1 + \gamma)}{\Gamma(1 + \gamma) + k_{\text{nr}} + k_{\text{m}}} \quad (10)$$

$$\tau_{\text{m}} = \frac{1}{\Gamma + \Gamma_{\text{m}} + k_{\text{nr}} + k_{\text{m}}} = \frac{1}{\Gamma(1 + \gamma) + k_{\text{nr}} + k_{\text{m}}} \quad (11)$$

where Γ_{m} and k_{m} are radiative and nonradiative rates induced by metal. Because the concentration of dye on the silver/silica film was not dependent on the silver thickness, the ratio of the quantum yield Q_{m}/Q_0 was regarded to be approximately equal to the ratio of fluorescence intensity I_{m}/I_0 ($I_{\text{m}}/I_0 = \text{enhancement}$

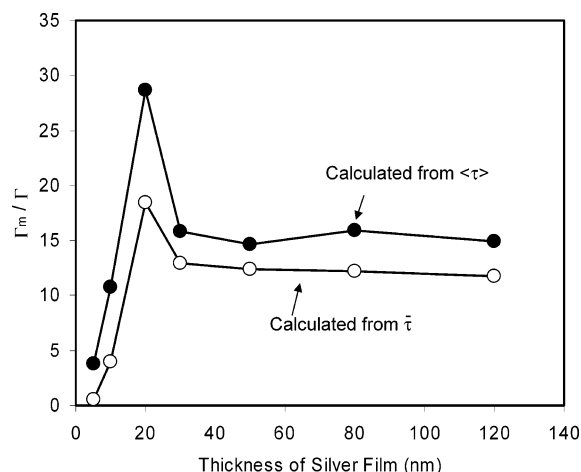


Figure 5. Correlation between the ratio of the radiative rate of a fluorophore on the metal film/glass substrate (Γ_{m}/Γ) and the thickness of the silver film.

factor). By combination of eqs 8–11, the dependence of Γ_{m}/Γ on I_{m}/I_0 could be written as eq 12.

$$\frac{Q_{\text{m}}}{Q_0} = \frac{l_{\text{m}}}{l_0} = \frac{\tau_{\text{m}}}{\tau_0} \left(1 + \frac{\Gamma_{\text{m}}}{\Gamma} \right) \quad (12)$$

According to eq 12, Γ_{m}/Γ were calculated using I_{m}/I_0 and $\langle \tau_{\text{m}} \rangle / \langle \tau_0 \rangle$ or $\bar{\tau}_{\text{m}} / \bar{\tau}_0$ (some data were listed in Table 1). Although the calculated values from $\langle \tau_{\text{m}} \rangle / \langle \tau_0 \rangle$ or $\bar{\tau}_{\text{m}} / \bar{\tau}_0$ were different, the change tendency with the thickness of silver film was similar (Figure 5). Most Γ_{m}/Γ values were larger than 1, indicating that the radiative rate of fluorophore on the metal film was faster than that on the glass substrate. The value increased with the thickness of silver film and then decreased, showing the maximum at 20 nm silver film thickness. Considering that Γ was a constant independent of the silver thickness, the Γ_{m} value should have its maximum at 20 nm, which was consistent with the saturation enhancement factor. Hence, Γ_{m} was regarded as the most important factor to contribute the MEF.

The dependence of MEF on the emission wavelength was studied by binding different dye-labeled anti-rabbit IgGs, including Rhodamine 6G, Alexa Fluor-647, Alexa Fluor-680, and Alexa Fluor-750, to the immobilized rabbit IgG on the silver film. The silver film (10 nm thick, deposited at 0.1 nm/10 s) was coated with a 5 nm thickness of silica. According to the luminescence intensity change of the fluorophore in the buffer solution before and after binding as well as the direct surface luminescence (Figure 6), it was inferred that all kinds of dye-labeled anti-rabbit IgGs did bind to the Rabbit IgG on the silica. The surface luminescence spectra were excited at 510, 565, 590, and 660 nm, and the excitation wavelengths were collected at 557, 635, 678, and 736 nm, respectively. The enhancement factor was found to rely on the emission wavelength (Figure 7). The luminescence intensity was enhanced ca. 3 times in the visible region of 550–650 nm, and then the enhancement factor increased to 5.3 with the wavelength, red-shifting to the near-IR region. The mechanism of the wavelength dependence of MEF is uncertain, but the low intensity of plasmon absorbance from the silver film in the near-IR region, which should weaken absorptions of the excitation and emission wavelengths of the fluorophore, was a probable reason.³⁰ This result implied that the fluorophore in the near-IR region could provide a more sensitive analysis in the fluoroimmunoassay when using the MEF technique.

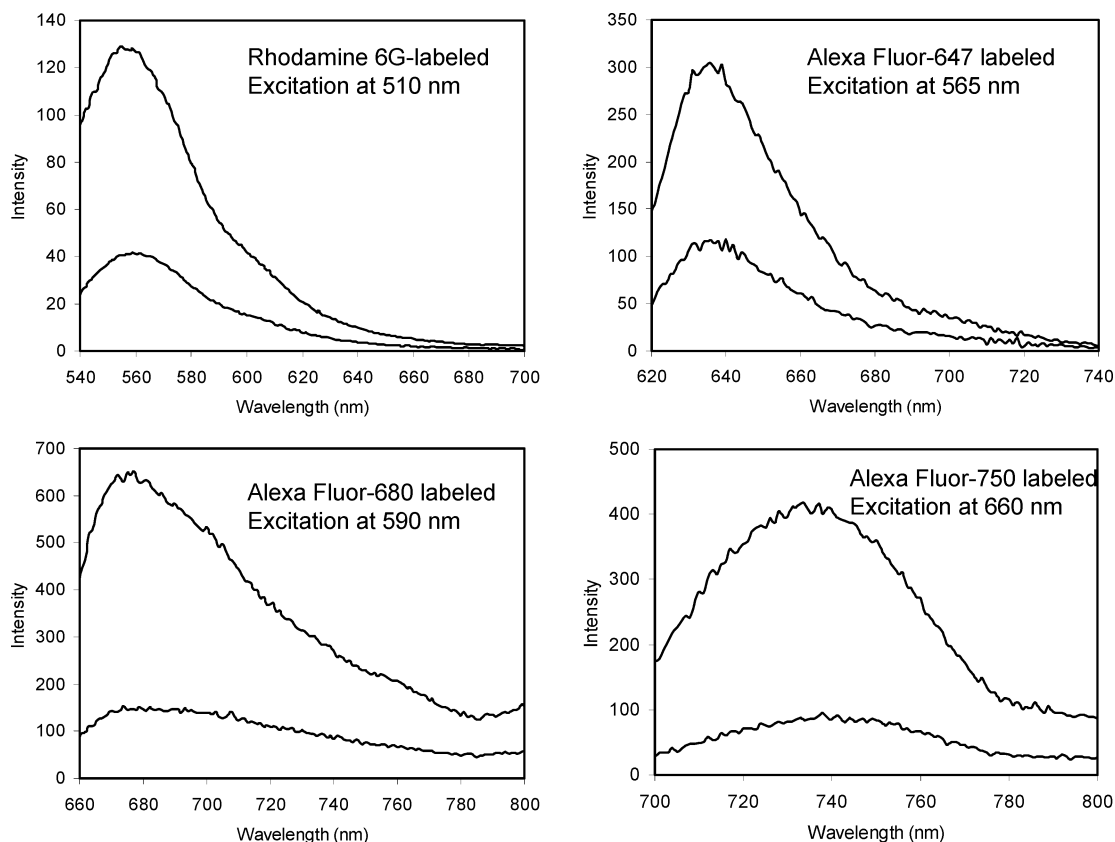


Figure 6. Surface emission spectra of four kinds of fluorophore-labeled antibody on a 10 nm thickness of a silver film coated by a 5 nm thickness of silica.

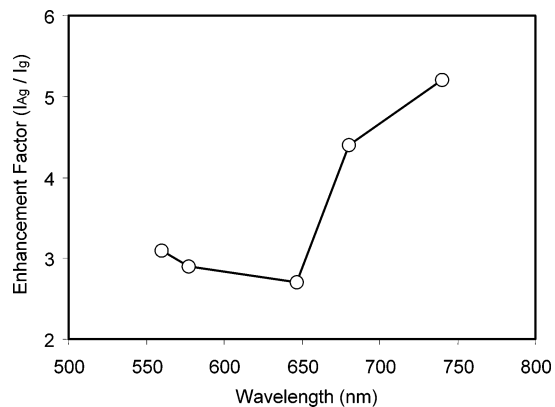


Figure 7. Dependence of the enhancement factor on the emission wavelength of a fluorophore-labeled antibody on a 10 nm thickness of a silver film coated by a 5 nm thickness of silica.

Summary

Silver film was grown on a glass substrate by vapor deposition at a slow rate (0.1 nm/10 s) and then covered by silica. The thin silver film (<20 nm) was composed of nanoparticles, while the thick silver film (>20 nm) became continuous and its surface was rough. The thin silver film displayed a plasmon absorbance at 490–650 nm depending on the thickness, implying that the particle size became large with increasing the thickness of silver film. This point was verified by AFM images. A model fluoroimmunoassay was performed on the silver film. Rabbit immunoglobulin G (IgG) was adsorbed on the silica by physisorption, and dye-labeled anti-rabbit IgG was bound to the immobilized IgG. When the Alexa Fluor-555 anti-rabbit IgG was employed, the surface fluorescence on the silver film was enhanced relative to that on the glass substrate, except a very

thin film (ca. 2 nm), and the enhancement factor increased with the thickness of silver film. The MEF reached saturation at a 20 nm thickness of silver film. The shortest lifetime at 20 nm silver film suggested that the MEF occurred by a mechanism of increasing radiative rate for the fluorophore induced on the metal. The silver film (10 nm) was coated by varying thicknesses of silica to study the dependence of MEF on the distance between the fluorophore and silver surface. The maximum enhancement occurred at a 10 nm thickness of silica and became very weak at 50 nm. The lifetime was shortest at a 10 nm thickness of silica, became longer with increasing the thickness of silica, and was close to that on the glass substrate at 50 nm. Therefore, the conditions for the strongest MEF in this model fluoroimmunoassay were proposed to occur with a 20 nm thickness of silver and a 10 nm thickness of silica. The dependence of MEF on the emission wavelength was studied through binding different dye-labeled anti-rabbit IgGs to the immobilized IgG, showing that the fluorescence in the near-IR region could be enhanced more efficiently than that in the visible region for the fluoroimmunoassay analysis.

Acknowledgment. This research was supported by grants from the National Center for Research Resources (RR08119) and National Human Genome Research Institute (HG02655) of the National Institutes of Health.

References and Notes

- (1) Pickup, J. C.; Thevenot, D. R. In *Advances in Biosensors*; JAI Press: London, UK, 1993; Suppl. 1.
- (2) (a) *Frontiers in Biosensorics I. Fundamental Aspects*; Scheller, F. W., Schubert, F., Fedrowitz, J., Eds.; Birkhauser Verlag: Berlin, 1997. (b) *Frontiers in Biosensorics II. Practical Applications*; Scheller, F. W., Schubert, F., Fedrowitz, J., Eds.; Birkhauser Verlag: Berlin, 1997.
- (3) Lakowicz, J. R.; Emerging Biomedical Application of Time-Resolved Fluorescence Spectroscopy. In *Probe Design and Chemical*

Sensing; Lakowicz, J. R., Ed.; Topics in Fluorescence Spectroscopy; Plenum Press: New York, 1994; Vol. 4, pp 1–9.

(4) (a) Gryczynski, I.; Malicka, J.; Shen, Y. B.; Gryczynski, Z.; Lakowicz, J. R. *J. Phys. Chem. B* **2002**, *106*, 2191. (b) Gryczynski, I.; Malicka, J.; Shen, Y. B.; Gryczynski, Z.; Lakowicz, J. R. *J. Phys. Chem. B* **2002**, *106*, 2191.

(5) (a) Malicka, J.; Gryczynski, I.; Gryczynski, Z.; Lakowicz, J. R. *Anal. Biochem.* **2003**, *315*, 57. (b) Malicka, J.; Gryczynski, I.; Gryczynski, Z.; Lakowicz, J. R. *J. Biomed. Opt.* **2003**, *8*, 472. (c) Malicka, J.; Gryczynski, I.; Fang, J.; Kusba, J.; Lakowicz, J. R. *Anal. Biochem.* **2003**, *315*, 160.

(6) Lakowicz, J. R. *Anal. Biochem.* **2001**, 298, 1.

(7) (a) Sokolov, K.; Chumanov, G.; Cotton, T. M. *Anal. Chem.* **1998**, *70*, 3898. (b) Chumanov, G.; Sokolov, K.; Gregory, B. W.; Cotton, T. M. *J. Phys. Chem.* **1995**, *99*, 9466.

(8) Geddes, C. D.; Cao, H.; Gryczynski, I.; Gryczynski, Z.; Fang, J. Y.; Lakowicz, J. R. *J. Phys. Chem. A* **2003**, *107*, 3443.

(9) (a) Geddes, C. D.; Parfenov, A.; Roll, D.; Fang, J. Y.; Lakowicz, J. R. *Langmuir* **2003**, *19*, 6236. (b) Parfenov, A.; Gryczynski, I.; Malicka, J.; Geddes, C. D.; Lakowicz, J. R. *J. Phys. Chem. B* **2003**, *107*, 8829.

(10) Evanoff, D. D.; White, R. L.; Chumanov, G. *J. Phys. Chem. B* **2004**, *108*, 1522.

(11) Messinger, B. J.; von Raben, K. U.; Chang, R. K.; Barber, P. W. *Phys. Rev. B* **1981**, *24*, 649.

(12) Lakowicz, J. R. *Anal. Biochem.* **2005**, 337, 171.

(13) Kreibig, U.; Vollmer, M. *Optical Properties of Metal Clusters*; Springer-Verlag: Berlin and Heidelberg, Germany, 1995.

(14) Feldheim, D. L.; Foss, C. A. *Metal Nanoparticles. Synthesis, Characterization and Applications*; Marcel Dekker: New York, 2002.

(15) Kerker, M.; Blatchford, C. G. *Phys. Rev. B* **1982**, *26*, 4082.

(16) *Luminescence Immunoassay and Molecular Applications*; Van Dyke, K., Van Dyke, K., Eds.; CRC Press: Boca Raton, FL, 1990.

(17) Hemmila, I. A. *Application of Fluorescence in Immunoassays*; John Wiley & Sons: New York, 1992.

(18) Vo-Dinh, T.; Sepaniak, M. J.; Griffin, G. D.; Alarie, J. P. *ImmunoMethods* **1993**, *3*, 85.

(19) Matveeva, E.; Gryczynski, Z.; Malicka, J.; Gryczynski, I.; Lakowicz, J. R. *Anal. Biochem.* **2004**, *334*, 303.

(20) Schlegel, V. L.; Cotton, T. M. *Anal. Chem.* **1991**, *63*, 241.

(21) Leverette, C. L.; Shubert, V. A.; Wade, T. L.; Varazo, K.; Dluhy, R. A. *J. Phys. Chem. B* **2002**, *106*, 8747.

(22) Van Duyne, R. P.; Hulteen, J. C.; Treichel, D. A. *J. Chem. Phys.* **1993**, *99*, 2101.

(23) Saito, Y.; Wang, J. J.; Smith, D. A.; Batchelder, D. N. *Langmuir* **2002**, *18*, 2959.

(24) Roark, S. E.; Semin, D. J.; Rowlen, K. L. *Anal. Chem.* **1996**, *68*, 473.

(25) Khriachtchev, L.; Heikkila, L.; Kuusela, T. *Appl. Phys. Lett.* **2001**, *78*, 1994.

(26) Zhang, Z. J.; Imae, T. *J. Colloid Interface Sci.* **2001**, 233, 99.

(27) (a) Haynes, C. L.; McFarland, A. D.; Smith, M. T.; Hulteen, J. C.; Van Duyne, R. P. *J. Phys. Chem. B* **2002**, *106*, 1898. (b) Dick, L. A.; McFarland, A. D.; Haynes, C. L.; Van Duyne, R. P. *J. Phys. Chem. B* **2002**, *106*, 853.

(28) Hansma, H. G.; Vesenka, J.; Siergerist, C.; Kelderman, G.; Morrett, H.; Sinzheimer, R. L.; Elings, V.; Bustamante, C.; Hansma, P. K. *Science* **1992**, 256, 1180.

(29) Shabert, F. A.; Rabe, J. P. *Biophys. J.* **1996**, *70*, 1514.

(30) Aguila, A.; Murray, R. W. *Langmuir* **2000**, *16*, 5949.